Journal of Solid State Chemistry **153,** 158–169 (2000)
doi:10.1006/jssc.2000.8767, available online at http://www.idealibrary.com on IDEAL®

Flux Synthesis and Isostructural Relationship of Cubic $Na_{1.5}Pb_{0.75}PSe_4$, $Na_{0.5}Pb_{1.75}GeS_4$, and $Li_{0.5}Pb_{1.75}GeS_4$

Jennifer A. Aitken,* Gregory A. Marking,* Michel Evain,† Lykourgos Iordanidis,* and Mercouri G. Kanatzidis*

*Department of Chemistry and Center for Fundamental Materials Research, Michigan State University, East Lansing, Michigan 48824; and †IMN, UMR CNRS C6502, Institut des Matériaux Jean Rouxel, Laboratoire de Chimie des Solides, 2 rue de la Houssinière, BP 32229, 44322 Nantes Cedex 03, France

Received February 3, 2000; in revised form May 8, 2000; accepted May 11, 2000; published online July 7, 2000

$Na_{1.5}Pb_{0.75}PSe_4$ was synthesized by the reaction of Pb with a molten mixture of $Na_2Se/P_2Se_5/Se$ at 495°C. $Na_{0.5}Pb_{1.75}GeS_4$ was synthesized by reacting Pb and Ge in molten Na_2S_x at 530°C. Likewise, $Li_{0.5}Pb_{1.75}GeS_4$ can be synthesized in a Li_2S_x flux at 500°C. $Na_{0.5}Pb_{1.75}GeS_4$ and $Li_{0.5}Pb_{1.75}GeS_4$ are relatively air- and water-stable, while $Na_{1.5}Pb_{0.75}PSe_4$ is only stable in air and water for less than 1 day. The structures of all three compounds were determined by single-crystal X-ray diffraction. The compounds crystallize in the cubic, noncentrosymmetric space group $I\bar{4}3d$ with $a = 14.3479(2)$ Å, $Z = 16$, $R1 = 0.0226$, and $wR2 = 0.0517$ for $Na_{1.5}Pb_{0.75}PSe_4$, $a = 14.115(1)$ Å, $Z = 16$, $R1 = 0.0284$, and $wR2 = 0.0644$ for $Na_{0.5}Pb_{1.75}GeS_4$, and $a = 14.0163(6)$ Å, $Z = 16$, $R1 = 0.0273$, and $wR2 = 0.0637$ for $Li_{0.5}Pb_{1.75}GeS_4$. The compounds adopt a structure that is similar to that of $Ba_3CdSn_2S_8$ and feature $[PSe_4]^{3-}$ or $[GeS_4]^{4-}$ tetrahedral building blocks. In this three-dimensional structure, there are two types of metal sites. In each structure, these sites are occupied differently because of a disorder between the alkali and lead cations. All three compounds are semiconductors with band gaps around 2 eV. The observation of a large second harmonic generation (SHG) signal for $Na_{0.5}Pb_{1.75}GeS_4$ indicates that it may be a potential nonlinear optical (NLO) material. Infrared and Raman spectroscopic characterization is also reported.

Key Words: **chalcogenides; second harmonic generation; molten salt fluxes; selenophosphate; thiogermanate.**

INTRODUCTION

The application of molten alkali metal polychalcogenide fluxes in the past decade has contributed a great deal to the synthetic chemistry of ternary and quaternary chalcogenides (1–4). More recently, this flux method has been modified and extended to address the solid state chemistry of multinary thio- and selenophosphates (5). The use of a polychalcophosphate flux involves the *in-situ* generation of well-defined, discrete $[P_xQ_y]^{n-}$ anionic fragments, which are the building blocks required to form chalcophosphate solids. These anionic species can become solubilized in an excess of polychalcogenide flux and then coordinate to metal cations to form molecular, (6–9), one-dimensional (6, 8, 10–14), two-dimensional (6, 11, 15–19), and three-dimensional compounds (7, 19–21). Prior to the use of fluxes to prepare new thio- and selenophosphates, the state of development in this class of materials was limited mostly to the $M_2P_2Q_6$ (Q = S, Se) family and some other ternary solids. A few of these compounds have been investigated for their nonlinear optical properties (22), ferroelectric applications (23), ion-exchange capacity (24), and luminescent behavior (25). The structures and properties of these materials underscore a great potential with respect to learning new chemistry and physics from investigating these types of materials.

We have now extended this work from chalcophosphates to chalcogermanates and chalcostannates. Because the $[M_xQ_y]^{z-}$ (M = Ge, Sn; Q = S, Se) anions are more highly charged than the $[P_xQ_y]^{n-}$ anions, the structures are expected to be different because of different charge-balancing requirements. Further investigations into these compounds promise to expose a comparably rich chemistry (26–28).

In combination with selenophosphate and thiogermanate anions we have explored the reactivity of Pb which gave rise to $APbPSe_4$ (A = Rb, Cs), $A_4Pb(PSe_4)_2$ (A = Rb, Cs) (11), $Rb_2PbGe_2S_6$, $K_2PbGe_2S_6$, $K_2Pb_3Ge_3S_{10}$, and $Cs_4Pb_4Ge_5S_{16}$ (29). Later, we examined these systems using the corresponding sodium and lithium chalcogenide fluxes. These fluxes are more challenging because as the size of the alkali metal decreases, the basicity decreases along with the probability that the alkali metal will be incorporated into the final product (2). Yet, this proved successful in synthesizing $Na_8Pb_2[Ge_2S_6]_2$ (26) and recently $Na_{1.5}Pb_{0.75}PSe_4$, $Na_{0.5}Pb_{1.75}GeS_4$, and $Li_{0.5}Pb_{1.75}GeS_4$, which are isostructural and reported here.

$Na_{1.5}Pb_{0.75}PSe_4$, $Na_{0.5}Pb_{1.75}GeS_4$, and $Li_{0.5}Pb_{1.75}GeS_4$ could not be made in pure form via direct combination

0022-4596/00 $35.00

reactions of the elements or the binary chalcogenides; they are products which seem to be stabilized only in the flux. These compounds adopt a cubic structure, which is similar to that of $Ba_3CdSn_2S_8$ and $Ba_6CdAg_2Sn_4S_{16}$ (30); however, they exhibit some disorder between the lead and alkali cations. Spectroscopic characterization is also reported.

EXPERIMENTAL SECTION

Reagents

The chemicals in this work were used as obtained: (i) sodium metal, analytical reagent, Mallinckrodt Inc. (Paris, KY); (ii) lithium metal rods, 99.9%, 12.7 mm diameter (Aldrich Chemical Co., Inc., Milwaukee, WI); (iii) lead metal powder, 200 mesh (Spectrum, Gardena, CA); (iv) germanium metal powder 99.999%, 100 mesh (Alfa-Aesar, Ward Hill, MA); (v) red phosphorus powder, 100 mesh (EM Science, Gibbstown, NJ); (vi) sulfur powder, sublimed (Spectrum, Gardena, CA); (vii) selenium powder 99.5 + %, 100 mesh (Aldrich Chemical Co., Inc., Milwaukee, WI); (viii) *N*,*N*-dimethylformamide 99.8%, A.C.S. reagent (Aldrich Chemical Co., Inc., Milwaukee, WI); (ix) diethyl ether, ACS Grade, anhydrous (Columbus Chemical Industries, Inc., Columbus, WI).

Synthesis

A_2Q (A = Li or Na; Q = S or Se). Li_2S, Na_2S, and Na_2Se were prepared using a modified literature procedure (31, 32).

PbS. A 10.34 g (0.05 mol) amount of Pb was combined with 1.60 g (0.05 mol) of S and loaded into a quartz tube. The tube was heated to 700°C in 24 h. It was kept at 700°C for 144 h and then cooled 65°C/h to 50°C. The gray/silver microcrystalline product was ground and bottled.

P_2Se_5. The amorphous phosphorus selenide glass, "P_2Se_5," was prepared by heating 4.068 g (0.131 mol) of P and 25.930 g (0.328 mol) of Se powder in an evacuated Pyrex ampoule for 24 h at 460°C. The glass was ground up and stored in a nitrogen-filled glovebox.

Preparation of $Na_{1.5}Pb_{0.75}PSe_4$. In a nitrogen-filled glovebox, 0.187 g (0.9 mmol) of Pb, 0.274 g (0.6 mmol) of P_2Se_5, 0.113 g (0.9 mmol) of Na_2Se, and 0.071 g (0.9 mmol) of Se were loaded into a Pyrex tube. The tube was flame-sealed under vacuum (approximately 2×10^{-4} mbar) and inserted into a programmable furnace. The temperature was raised from 50°C to 540°C in 24 h. It was kept at 540°C for 30 h and then cooled 3°C/h to 300°C followed by cooling 50°C/h to 50°C. The product was isolated by washing away the excess flux with *N*,*N*-dimethylformamide and washed with ether. The products were red plates and polyhedra and silver polyhedra (60%/40% yield). Semiquantitative energy dispersive analysis (EDS) using a scanning electron microscope (SEM) on a number of the red plates and red polyhedra indicated the presence of all four elements. The powder diffraction pattern of the red plates and red polyhedra indicated a new phase. The powder diffraction pattern of the gray polyhedra was indexed to PbSe.

Preparation of $Na_{0.5}Pb_{1.75}GeS_4$. In a nitrogen-filled glovebox, 0.052 g (0.25 mmol) of Pb, 0.054 g (0.75 mmol) of Ge, 0.039 g (0.50 mmol) of Na_2S, and 0.064 g (2 mmol) of S were loaded into a Pyrex tube. The Pyrex tube was flame-sealed under vacuum (approximately 2×10^{-4} mbar) and inserted into a programmable furnace. The temperature was raised from 50°C to 530°C in 20 h. It was kept at 530°C for 34 h, and then cooled 5°C/h to 50°C. *N*,*N*-Dimethylformamide was used to remove the excess flux, and washing with ether revealed small orange/red crystals as a pure phase. The presence of all four elements was detected in several of the crystals with semiquantitative EDS using a SEM. The powder diffraction pattern indicated a new phase.

Preparation of $Li_{0.5}Pb_{1.75}GeS_4$. In a nitrogen-filled glovebox 0.093 g (0.45 mmol) of Pb, 0.022 g (0.3 mmol) of Ge, 0.007 g (0.15 mmol) of Li_2S, and 0.077 g (2.4 mmol) of S were loaded into a graphite tube. The graphite tube was inserted into a 13 mm Pyrex tube and flame-sealed under vacuum (approximately 2×10^{-4} mbar). The Pyrex tube was then placed into a programmable furnace and heated from 50°C to 500°C in 24 h. The reaction was kept at this temperature for 96 h and then cooled at 2.5°C per hour to 250°C followed by rapid cooling to 50°C in 2 h. The product was isolated as described above as pure orange/red crystalline chunks. Analysis of the small orange/red chunks using semiquantitative EDS attached to a SEM indicated the presence of Pb, Ge, and S (lithium cannot be detected by EDS). Analysis preformed using inductively coupled plasma (ICP) confirmed the presence of Li, Pb, and S in a 0.57:1.73:4 molar ratio (there was no standard made for germanium). The powder diffraction pattern indicated a new phase. In order to obtain crystals suitable for single-crystal X-ray diffraction, the same starting mixture was loaded into a graphite tube. The graphite tube was inserted into a 13 mm quartz tube and flame-sealed under vacuum (approximately 2×10^{-4} mbar). This tube was heated from 50°C to 650°C in 12 h. The reaction was kept at this temperature for 72 h and then cooled at 2.75°C per hour to 250°C followed by rapid cooling to 50°C in 2 h. The product was isolated in the same manner as previous to reveal beautiful, red plate-like single crystals as a pure phase.

Physical Measurements

Powder X-ray diffraction. Analyses were performed using a calibrated Rigaku-Denki/RW400F2 (Rotaflex) rotating anode powder diffractometer controlled by an IBM

computer, operating at 45 kV/100 mA and with a 1°/min scan rate, employing Ni-filtered Cu radiation in Bragg–Brentano geometry. Powder patterns were calculated with the Cerius[2] software package (33).

Electron microscopy. Quantitative microprobe analysis of the compounds were performed with a JEOL JSM-6400V SEM equipped with a Noran Vantage EDS detector. Data were acquired with an accelerating voltage of 25 kV and a 40 s accumulation time.

Inductively coupled plasma spectroscopy (ICP). Samples were submitted to the Animal Health Diagnostics Laboratory at Michigan State University for analysis. Experiments were carried out on a Thermo Jarrel Ash Polyscan 61E Simultaneous/Sequential inductively coupled plasma-atomic emission spectrometer (ICP-AES) with vacuum spectrometers and Ar-purged optical paths. The solid powders were weighed onto an analytical balance and then digested in a Teflon container in concentrated nitric acid overnight at 95°C. The digest was transferred to a 25 ml volumetric flask and diluted with water. Yttrium was used as an internal standard in 2% HNO_3. Multielemental analyses were done by nebulizing the liquid sample into an argon flame (plasma) that was sustained by a surrounding high-frequency magnetic field. The photons emitted are collimated and directed by a diffraction grating onto a semicircular array of photomultiplier tubes, one for each element to be measured. A computer then converts the photomultiplier signals to concentration units.

Differential thermal analysis (DTA). Differential thermal analysis (DTA) was performed with a computer-controlled Shimadzu DTA-50 thermal analyzer. Approximately 20 mg of the samples were sealed in a carbon-coated quartz ampoule under vacuum. A quartz ampoule containing alumina of equal mass was sealed and placed on the reference side of the detector. The sample was heated to 800°C at 10°C/min, isothermed for 5 min, and then cooled at a rate of 10°C/min to 100°C, followed by rapid cooling to room temperature. Residues of the DTA experiments were examined by powder X-ray diffraction. The stability and reproducibility of the samples were monitored by running multiple heating and cooling cycles.

Single-crystal UV/vis spectroscopy. Optical transmission measurements were made at room temperature on single crystals using a Hitachi U-6000 microscopic FT spectrophotometer with an Olympus BH-2 metallurgical microscope over a range of 380–900 nm.

Solid-State UV/vis/near IR spectroscopy. Optical diffuse reflectance measurements were performed at room temperature using a Shimadzu UV-3101PC double-beam, double-monochromator spectrophotometer. The instrument is equipped with an integrating sphere and controlled by a personal computer. $BaSO_4$ was used as a 100% reflectance standard. The sample was prepared by grinding the crystals to a powder and spreading them on a compacted surface of the powdered standard material, preloaded into a sample holder. The reflectance versus wavelength data generated were used to estimate the band gap of the material by converting reflectance to absorption data (34).

Infrared spectroscopy. FT-IR spectra were recorded as solids in a CsI matrix. The samples were ground with dry CsI into a fine powder and pressed into translucent pellets. The spectra were recorded in the far-IR region (600–100 cm^{-1}, 4 cm^{-1} resolution) with the use of a Nicolet 740 FT-IR spectrometer equipped with a TGS/PE detector and silicon beam splitter.

Raman spectroscopy. Raman spectra were recorded on a Holoprobe Raman Spectrograph equipped with a 633 nm HeNe laser and a CCD camera detector. The instrument was coupled to an Olympus BX60 microscope. For each sample, crystals were simply placed onto a small glass slide and a 50× objective lens was used to choose the area of the crystal specimens to be measured. The spot size of the laser beam when using the 50× objective lens was 10 μm.

Single-Crystal X-Ray Crystallography

$Na_{1.5}Pb_{0.75}PSe_4$. A plate-like crystal with dimensions $0.16 \times 0.09 \times 0.03\ mm^3$ was mounted on a glass fiber. A Bruker SMART Platform CCD diffractometer, operating at 50 kV/40 mA and using graphite-monochromatized Mo$K\alpha$ radiation, was used for data collection. No initial cell is needed to collect data using this procedure. A full sphere of data was collected in three major swaths of frames with 0.30° steps in ω and an exposure time of 45 s per frame. Crystal stability was determined at the end of the data collection by recollecting the first 50 frames of the data and comparing them to the original first 50 frames. No crystal decay was detected. An initial cell was obtained by with the SMART (35) program to extract reflections from the frames of the actual data collection. This orientation matrix was used to integrate the data with the SAINT (35) program. The final cell constants were determined from a set of 6673 strong reflections obtained from data collection.

An empirical absorption correction was done using SADABS (36), and all refinements were done with the SHELXTL (37) package of crystallographic programs. The systematic absences pointed clearly to the space group $I\bar{4}3d$. One lead, one sodium, one phosphorus, and two selenium atoms were found in special positions except for one of the selenium atoms. However, the thermal displacement parameter, U(eq), of Pb(1) was high (0.046 $Å^2$), and the thermal displacement parameter of the sodium atom, which we will call Na(2), was also high (0.048 $Å^2$) compared to that of the

other atoms ($R1 = 10.5\%$ w$R2 = 29\%$). For the Pb(1) position, a disorder model was applied by introducing another atom, Na(1), so that the sum of the occupancies was set equal to full occupancy. Na(2) was found to generate a symmetry-equivalent position ~ 0.8 Å from itself. This position was then constrained to be half-occupied. After least-squares refinement, the disorder site between Pb(1) and Na(1) refined to 49.4% Pb(1) and 50.6% Na(1), the thermal displacement parameter of the Pb(1)/Na(1) site dropped to 0.027 Å^2, and the Na(2) position had a reasonable thermal displacement parameter (0.024 Å^2) ($R1 = 4.3\%$ w$R2 = 14.8\%$). The Pb(1)/Na(1) site was constrained to 50%/50%, which gave a charged-balanced formula and after refinement, no change in the R values was noted. Next, all the atoms were refined anisotropically except for Na(2) ($R1 = 2.26\%$, w$R2 = 5.17\%$). Refining Na(2) anisotropically was not deemed statistically significant. The maximum and minimum peaks on the final Fourier difference map corresponded to 1.134 and -0.781 e$^-$/Å^3. Crystallographic data for $Na_{1.5}Pb_{0.75}PSe_4$ are given in Table 1, and fractional atomic coordinates and anisotropic temperature factors are in Tables 2 and 3.

$Na_{0.5}Pb_{1.75}GeS_4$. A block-like crystal having dimensions ca. $0.10 \times 0.10 \times 0.05$ mm^3 was glued at the tip of a Lindemann glass capillary. The data collection was carried out on a P4 Siemens diffractometer. To avoid severe absorption effects and ease refinements, a graphite-monochromatized Ag radiation ($\lambda = 0.56087$ Å) was used. The orientation matrix and the cubic cell constant were obtained from the centering of 28 high θ value reflections. The intensities of all reflections but the Friedel pairs were collected in an ω scan mode. The intensity decay observed during the room temperature measurements was less than 1%.

The measured intensities were obtained by fitting of the reflection profiles. They were corrected for scale variations by means of three standard reflections. Data reduction, absorption corrections, and all refinements were carried out with the JANA98 program package (38). Prior to a Gaussian-type analytical absorption correction, an optimization of the crystal size and shape based upon ψ-scan measurements was performed with the X-Shape program (39). The 9713 reflection intensities were then merged according to the $I\bar{4}3m$ point group, with an internal R(obs) value of ca. 10.0% and an $I > 2\sigma(I)$ cutoff as a criterion for observed reflections.

Two lead, one germanium, and two sulfur atoms were found, all of which occupied special positions except for one of the sulfur atoms. After least-squares refinement, the atomic displacement parameter, U(eq) of Pb(2) was extremely high compared to that of the other atoms. When this position was assigned as sodium, the atomic displacement parameter was almost zero. This position was assigned as Pb(2) ($R1 = 13.0\%$, w$R2 = 31.8\%$), and it was found to generate a symmetry-equivalent position about 1 Å from itself. The occupancy was then constrained to be 50% occupied by Pb, which reduced the U(eq) of Pb(2) to 0.32 Å^2 as well as the $R1$ and w$R2$ values to 12.5% and 30.6%, respectively. At this stage, a sodium atom, Na(2), was found to be disordered with Pb(2). The sum of the occupancies was set equal to 50%, and after least-squares refinement the occupancy of Pb(2) dropped to 16.25% while the occupancy of Na(2) refined to 33.75%. The atomic displacement parameter of Pb(2)/Na(2) dropped dramatically to 0.040 Å^2, giving $R1 = 8.1\%$ and w$R2 = 20.3\%$. Because 16.7% lead gives a charge-balanced formula, the occupancy of Pb(2) was constrained to 16.7% and the occupancy of Na(2) was constrained to 33.3% with no change in the R values observed. All atoms were subsequently refined anisotropically, which considerably improved the residual factors ($R1 = 2.84\%$, w$R2 = 6.44\%$). Refining the Pb(1)/Na(1) site anisotropically was acceptable for this structure because the symmetry-equivalent position was about 1 Å away in this case as opposed to ca. 0.8 Å in the case of $Na_{1.5}Pb_{0.75}PSe_4$. The maximum and minimum peaks on the final Fourier difference map corresponded to 2.60 and -2.40 e$^-$/Å^3, respectively. Crystallographic data for $Na_{0.5}Pb_{1.75}GeS_4$ are given in Table 1, and fractional atomic coordinates and anisotropic temperature factors are in Tables 2 and 3.

TABLE 1
Crystallographic Data for $Na_{1.5}Pb_{0.75}PSe_4$, $Na_{0.5}Pb_{1.75}GeS_4$, and $Li_{0.5}Pb_{1.75}GeS_4$

Formula	$Na_{1.5}Pb_{0.75}PSe_4$	$Na_{0.5}Pb_{1.75}GeS_4$	$Li_{0.5}Pb_{1.75}GeS_4$
Formula weight	536.69	574.91	566.88
Crystal habit, color	Plate, red	Blocks, red	Plate, red
Space group	$I\bar{4}3d$ (#220)	$I\bar{4}3d$ (#220)	$I\bar{4}3d$ (#220)
a, Å	14.3479(2)	14.115(1)	14.0163(6)
Z; V, Å^3	16, 2953.69(7)	16, 2812.18(4)	16, 2753.6(2)
D(calcd), g/cm^{-3}	4.828	5.430	5.470
Temp, K	173	273	173
λ, Å	0.71073 (Mo$K\alpha$)	0.5609 (Ag$K\alpha$)	0.71073 (Mo$K\alpha$)
μ, mm^{-1}	37.078	25.6	48.131
F(000)	3664	3850	3856
θ_{max}, deg	27.09	27.25	30.55
Total data measd.	14,584	9,713	20,512
Total unique data	547[R(int) = 0.0919]	847 [R(int) = 0.102]	699 [R(int) = 0.0638]
No. of parameters	24	27	27
Refinement method	Full-matrix least-squares on F^2		
Final R indices ($I > 2\sigma(I)$)	$R1^a = 0.0226$ w$R2^b = 0.0517$	$R1 = 0.0284$ w$R2 = 0.0644$	$R1 = 0.0273$ w$R2 = 0.0637$
R indices (all data)	$R1 = 0.0252$ w$R2 = 0.0520$	$R1 = 0.0341$ w$R2 = 0.0660$	$R1 = 0.0314$ w$R2 = 0.0644$
Goodness of fit on F^2	1.187	0.99	1.141

$^a R1 = \sum||F_o| - |F_c||/\sum|F_o|$.
^{b}w$R2 = \{\sum[w(F_o^2 - F_c^2)^2]/\sum[w(F_o^2)^2]\}^{1/2}$.

TABLE 2
Atomic Coordinates and Equivalent Isotropic Displacement Parameters ($Å^2 \times 10^3$) for $Na_{1.5}Pb_{0.75}PSe_4$, $Na_{0.5}Pb_{1.75}GeS_4$, and $Li_{0.5}Pb_{1.75}GeS_4$

Atom	Wyckoff letter and multiplicity	x	y	z	U(eq)*	Occupancy
			$Na_{1.5}Pb_{0.75}PSe_4$			
Pb(1)[a]	24d	0.9923(1)	0.0000	0.7500	28(1)	0.5
Na(1)[a]	24d	0.9923(1)	0.0000	0.7500	28(1)	0.5
Na(2)[b]	24d	0.6535(5)	0.0000	0.7500	18(2)	0.5
P(1)	16c	0.7698(1)	0.7698(1)	0.7698(1)	12(1)	1.0
Se(1)	16c	0.9302(1)	0.9302(1)	0.9302(1)	20(1)	1.0
Se(2)	48e	0.8727(1)	0.6774(1)	0.8380(1)	16(1)	1.0
			$Na_{0.5}Pb_{1.75}GeS_4$			
Pb(1)[a]	24d	0.98842(3)	0.0000	0.7500	29.3(1)	1.0
Pb(2)[b]	24d	0.6612(2)	0.0000	0.7500	36.2(7)	0.167
Na(2)[b]	24d	0.6612(2)	0.0000	0.7500	36.2(7)	0.333
Ge(1)	16c	0.77614(5)	0.77614(5)	0.77614(5)	13.6(1)	1.0
S(1)	16c	0.9347(1)	0.9347(1)	0.9347(1)	13.7(3)	1.0
S(2)	48e	0.8758(2)	0.6779(2)	0.8469(2)	23.5(5)	1.0
			$Li_{0.5}Pb_{1.75}GeS_4$			
Pb(1)[a]	24d	0.0076(1)	0.0000	0.2500	23(1)	1.0
Pb(2)[b]	24d	0.3405(2)	0.0000	0.2500	23(1)	0.167
Li(2)[b]	24d	0.3405(2)	0.0000	0.2500	23(1)	0.333
Ge(1)	16c	0.2229(1)	0.2229(1)	0.2229(1)	10(1)	1.0
S(1)	16c	0.0654(1)	0.0654(1)	0.0654(1)	9(1)	1.0
S(2)	48e	0.1317(2)	0.3228(2)	0.1419(2)	27(1)	1.0

*U(eq) is defined as one-third of the trace of the orthogonalized $\mathbf{U}_{ij}$ tensor.

[a,b]The letters *a* and *b* are used to help the reader distinguish between the two 24*d* positions. "*a*" represents "cation site A." This position generates a symmetry-equivalent atom 3.807(2), 3.856(3), or 3.716(1) Å from itself. "*b*" represents "cation site B." This position generates a symmetry-equivalent atom 0.81(1), 1.021(4), or 0.968(6) Å from itself and is therefore half-occupied.

$Li_{0.5}Pb_{1.75}GeS_4$. A plate-like, $0.19 \times 0.03 \times 0.03\ mm^3$ crystal was mounted on a glass fiber. The data were collected using the same Bruker SMART CCD that was used for the data collection of $Na_{1.5}Pb_{0.75}PSe_4$. The same data collection and processing techniques used for $Na_{1.5}Pb_{0.75}PSe_4$ were utilized. The exposure time was 60 s per frame. No crystal decay was detected. The data were integrated using the same procedure as in $Na_{1.5}Pb_{0.75}PSe_4$. The final cell constants were determined from a set of 4427 strong reflections obtained from data collection.

$I\bar{4}3d$ was the space group chosen on the basis of the systematic absences. Two lead, one germanium, and two sulfur atoms were found, all of which occupied special positions except for one of the sulfur atoms. After least-squares refinement, the thermal displacement parameter, U(eq), of Pb(2) was extremely high (0.161 $Å^2$) compared to that of the other atoms ($R1 = 12.2\%$, w$R2 = 32.2\%$). This position was found to generate a symmetry-equivalent position about 1 Å from itself. Pb(2) was then constrained to be 50% occupied which reduced its thermal displacement parameter to 0.089 $Å^2$ as well as the $R1$ and w$R2$ values to 12.2% and 36.2%, respectively. At this stage, lithium atom, Li(2), was found to be disordered with Pb(2). The sum of the occupancies was set equal to 50% and after least-squares refinement the occupancy of Pb(2) dropped to 19% while the occupancy of Li(2) refined to 31%. The thermal displacement parameter of Pb(2)/Li(2) dropped dramatically to 0.027 $Å^2$, giving $R1 = 9.2\%$ and w$R2 = 30.5\%$. Since 16.7% lead gives a charge-balanced formula, the occupancy of Pb(2) was constrained to 16.7% and the occupancy of Na(2) was constrained to 33.3% with no change in the R values observed. All atoms were subsequently refined anisotropically ($R1 = 2.73\%$, w$R2 = 6.37\%$). Refining the Pb(2)/Li(2) site anisotropically was acceptable for this structure because the data were collected to a higher resolution and the symmetry-equivalent position was about 1 Å away in this case as opposed to ca. 0.8 Å in the case of $Na_{1.5}Pb_{0.75}PSe_4$. The maximum and minimum peaks on the final Fourier difference map corresponded to 1.633 and $-0.984\ e^-/Å^3$, respectively. Crystallographic data for $Li_{0.5}Pb_{1.75}GeS_4$ are given in Table 1, and fractional atomic coordinates and anisotropic temperature factors are in Tables 2 and 3.

TABLE 3
Anisotropic Displacement Parameters* ($Å^2 \times 10^3$) for $Na_{1.5}Pb_{0.75}PSe_4$, $Na_{0.5}Pb_{1.75}GeS_4$, and $Li_{0.5}Pb_{1.75}GeS_4$

Atom	U_{11}	U_{22}	U_{33}	U_{23}	U_{13}	U_{12}
			$Na_{1.5}Pb_{0.75}PSe_4$			
Pb(1)[a]	24(1)	36(1)	23(1)	2(1)	0	0
Na(1)[a]	24(1)	36(1)	23(1)	2(1)	0	0
P(1)	12(1)	12(1)	12(1)	−1(1)	−1(1)	−1(1)
Se(1)	20(1)	20(1)	20(1)	−4(1)	−4(1)	−4(1)
Se(2)	17(1)	16(1)	15(1)	−1(1)	−3(1)	5(1)
			$Na_{0.5}Pb_{1.75}GeS_4$			
Pb(1)[a]	22.0(2)	44.0(3)	22.0(2)	3.7(2)	0.0	0.0
Pb(2)[b]	61(1)	22(1)	26(1)	5(1)	0.0	0.0
Na(2)[b]	61(1)	22(1)	26(1)	5(1)	0.0	0.0
Ge(1)	13.6(5)	13.6(5)	13.6(5)	−0.5(2)	−0.5(2)	−0.5(2)
S(1)	13.7(5)	13.7(5)	13.7(5)	0.3(5)	0.3(5)	0.3(5)
S(2)	25.0(9)	19.4(8)	26.0(9)	6.1(7)	−11.4(7)	−2.8(7)
			$Li_{0.5}Pb_{1.75}GeS_4$			
Pb(1)[a]	13(1)	40(1)	15(1)	4(1)	0	0
Pb(2)[b]	48(2)	9(1)	10(1)	3(1)	0	0
Li(2)[b]	48(2)	9(1)	10(1)	3(1)	0	0
Ge(1)	10(1)	10(1)	10(1)	−1(1)	−1(1)	−1(1)
S(1)	9(1)	9(1)	9(1)	1(1)	1(1)	1(1)
S(2)	32(1)	13(1)	35(2)	1(1)	1(1)	1(1)

*The anisotropic displacement factor exponent takes the form $-2\pi^2[h^2a^{*2}U_{11} + k^2b^{*2}U_{22} + l^2c^{*2}U_{33} + 2hka^*b^*U_{12} + 2hla^*c^*U_{13} + 2klb^*c^*U_{23}]$.

[a,b]The letters *a* and *b* are used to help the reader distinguish between the two 24*d* positions. "*a*" represents "cation site A". This position generates a symmetry-equivalent atom 3.807(2), 3.856(3), or 3.716(1) Å from itself. "*b*" represents "cation site B". This position generates a symmetry-equivalent atom 0.81(1), 1.021(4), or 0.968(6) Å from itself and is therefore half-occupied.

RESULTS AND DISCUSSION

Synthesis

$Na_{1.5}Pb_{0.75}PSe_4$ was synthesized by reacting a mixture of Pb, P_2Se_5, Na_2Se, and Se in a 1.5:1.0:1.5:1.5 molar ratio at 495°C for 4 days. We were never able to make this compound pure. Although the best ratio to synthesize $Na_{1.5}Pb_{0.75}PSe_4$ was close to direct combination, it only formed in 60% yield. The other 40% of the isolated product was PbSe. Reactions that were richer in Na_2Se or Se gave more PbSe. Reactions at lower temperatures did not improve the synthesis, and reactions at higher temperatures only favored the formation of PbSe. $Na_{1.5}Pb_{0.75}PSe_4$ is only stable in air and water for less than 1 day. This compound features the $[PSe_4]^{3-}$ unit, whose occurrence in solid-state compounds is relatively uncommon. There are many more compounds containing the $[P_2Se_6]^{4-}$ unit, which suggests that the tetrahedral P^{5+} species is unstable with respect to the dimeric P^{4+} species under selenide-rich conditions. This is in contrast to the sulfide analogue, $[PS_4]^{3-}$, which tends to be much more prevalent relative to that of $[P_2S_6]^{4-}$. However, with the use of the selenophosphate flux and our ability to tune its properties, we have been able to stabilize the $[PSe_4]^{3-}$ unit a number of times (8, 11, 19, 40–42).

$Na_{0.5}Pb_{1.75}GeS_4$ was synthesized by reacting a mixture of Pb, Ge, Na_2S, and S in a 1:3:2:8 molar ratio at 530°C for 4 days. This compound could be synthesized relatively pure in the flux but could not be prepared in pure form by direct combination of the elements. Differential thermal analysis of the compound shows that $Na_{0.5}Pb_{1.75}GeS_4$ melts incongruently at 710°C. After melting, some of the compound recrystallizes while some decomposes to PbS and residual flux. $Na_{0.5}Pb_{1.75}GeS_4$ is air- and water-stable for at least a few years. $Li_{0.5}Pb_{1.75}GeS_4$ was synthesized by reacting a mixture of Pb, Ge, Li_2S, and S in a 3:2:1:16 molar ratio at 500°C for 4 days. The compound is similar in nature to its Na analogue. It melts incongruently at 668°C and slowly precipitates out PbS. $Li_{0.5}Pb_{1.75}GeS_4$ is air- and water-stable for a least a couple of weeks.

Structure

The cubic structure adopted by all three compounds is three-dimensional, noncentrosymmetric, and similar to that of $Ba_3CdSn_2S_8$ and $Ba_6CdAg_2Sn_4S_{16}$ (30). We will describe in detail the structure of $Na_{1.5}Pb_{0.75}PSe_4$ and then compare/contrast $Na_{0.5}Pb_{1.75}GeS_4$ and $Li_{0.5}Pb_{1.75}GeS_4$, respectively.

If one looks at the unit cell of $Na_{1.5}Pb_{0.75}PSe_4$ shown in Fig. 1, the structure seems to be rather complicated; however, when it is broken down into pieces, one can see things more clearly. The structure of $Na_{1.5}Pb_{0.75}PSe_4$ is made up of near-perfect $[PSe_4]^{3-}$ tetrahedral building blocks, with Se–P–Se bond angles of 107.14(8)° and 111.70(8)°. A view of only the tetrahedral building blocks, looking down the body diagonal, displayed in Fig. 2, shows that the structure is obviously noncentrosymmetric because all of the tetrahedra point in the same direction. These tetrahedral units coordinate to sodium or lead cations, which occupy two crystallographic sites in the structure. They are both special positions (24*d*) and will be referred to as cation site A and cation site B, corresponding to the numbering of the atoms which occupy these sites. Cation site A is disordered (50%/50%) between Na(1) and Pb(1). A symmetry-equivalent position is generated 3.807(2) Å away, see Fig. 3a, and can be described as a close contact. One can see in Fig. 3b the arrangement of the tetrahedral units surrounding this position. There are two Pb(1)/Na(1)–Se distances of 2.9124(3) Å and two distances of 3.054(1) Å. There are also four long Pb(1)/Na(1)–Se interactions, two of which are 3.4017(9) Å; the other two are 3.4385(9) Å, see Fig. 3c. Thus, when Pb(1) is in this position it can be considered to be 4-coordinate, with a distorted see-saw-like geometry, having

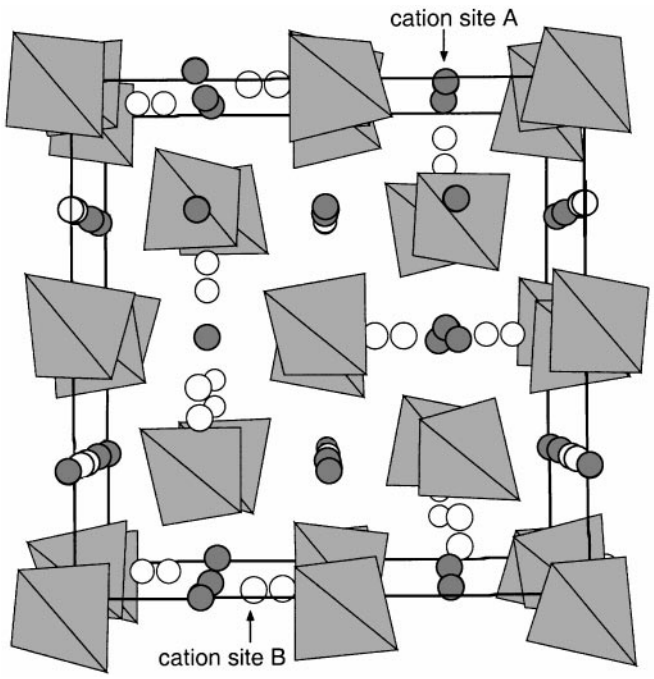

FIG. 1. Unit cell of $Na_{1.5}Pb_{0.75}PSe_4$. The $[PSe_4]^{3-}$ tetrahedral units are represented by gray polyhedra. Bonds between Pb and Se are omitted for clarity. Cation site A, the position that is disordered 50%/50% between Na and Pb, is shown in black, while the Na atoms, which sit on cation site B, are shown in white.

some additional long interactions. However, when Na(1) is in this position it can be considered as 8-coordinate since the interaction between Na and Se is less covalent and more ionic. Cation site B is occupied only by Na(2). The coordination environment of Na(2) is an irregular, 8-coordinate pocket shown in Fig. 4. This position generates a symmetry-equivalent atom 0.81(1) Å from itself, and therefore its maximum occupancy is 50%. Six of the Na(2)–Se distances range from 2.936(1) to 3.381(6) Å, while two are longer, 4.052(6) Å. See Tables 4 and 5 for additional distances and angles. The sites occupied by Na and/or Pb in these compounds are slightly larger than the sizes of both these cations, and a certain degree of "rattling" motion of these cations may be expected. If multiple equivalent energy minima exist within these cavities and if the positions of the Na and/or Pb ions in the 24*d* sites (see Table 2) could be influenced by the application of electric fields, then ferroelectric properties may be possible in these compounds.

$Na_{0.5}Pb_{1.75}GeS_4$ and $Li_{0.5}Pb_{1.75}GeS_4$ are isostructural to $Na_{1.5}Pb_{0.75}PSe_4$. They are both made up of $[GeS_4]^{4-}$ tetrahedral building blocks, with S–Ge–S bond angles of 105.40(8)° and 113.21(8)° for $Na_{0.5}Pb_{1.75}GeS_4$ and 105.39(7)° and 113.23(6)° for $Li_{0.5}Pb_{1.75}GeS_4$. These $[GeS_4]^{4-}$ tetrahedra are less perfect than the $[PSe_4]^{3-}$ tetrahedra found in $Na_{1.5}Pb_{0.75}PSe_4$. The $[GeS_4]^{4-}$ tetrahedral units are coordinated to lead and sodium or lithium atoms. As in $Na_{1.5}Pb_{0.75}PSe_4$ there are two metal sites which are special positions (24*d*) and referred to as cation sites A and B; however, they are now occupied differently. For both of the thiogermanates, cation site A is occupied only by Pb(1). This position generates a symmetry-equivalent atom 3.856(3) or 3.716(1) Å away, which corresponds to a weak Pb–Pb lone pair interaction (43). For $Na_{0.5}Pb_{1.75}GeS_4$, there are two Pb(1)–S bond distances of 2.846(2) Å and two of 2.867(2) Å, while there are four long interactions, two which are 3.443(2) Å and two which are 3.455(2) Å. For $Li_{0.5}Pb_{1.75}GeS_4$, there are two Pb(1)–S bond distances of 2.828(2) Å and two of 2.8623(6) Å, while there are four long interactions, two which are 3.403(2) Å and two which are 3.508(3) Å. Cation site B, in the case of both thiogermanates, is disordered between Na(2)/Li(2) and Pb(2) (33.3%/16.7%). This position generates a symmetry-equivalent atom 1.021(4) Å away in the case of $Na_{0.5}Pb_{1.75}GeS_4$ and 0.968(6) Å away for $Li_{0.5}Pb_{1.75}GeS_4$ and therefore can have a maximum occupancy of only 50%. In $Na_{0.5}Pb_{1.75}GeS_4$, there are four shorter Na(2)/Pb(2)–S distances: two are 2.806(2) Å, and two are 3.065(2) Å. Further out there exist two distances of 3.315(3) Å and two even longer distances of 3.716(1) Å. In the case of $Li_{0.5}Pb_{1.75}GeS_4$, there are four shorter Li(2)/Pb(2)–S distances two of which are 2.601(3) Å and two of which are 2.860(4) Å, while there are two longer distances of 3.496(4) Å and two even longer distances of 4.308(4). This site can be considered as a very large 8-coordinate pocket when

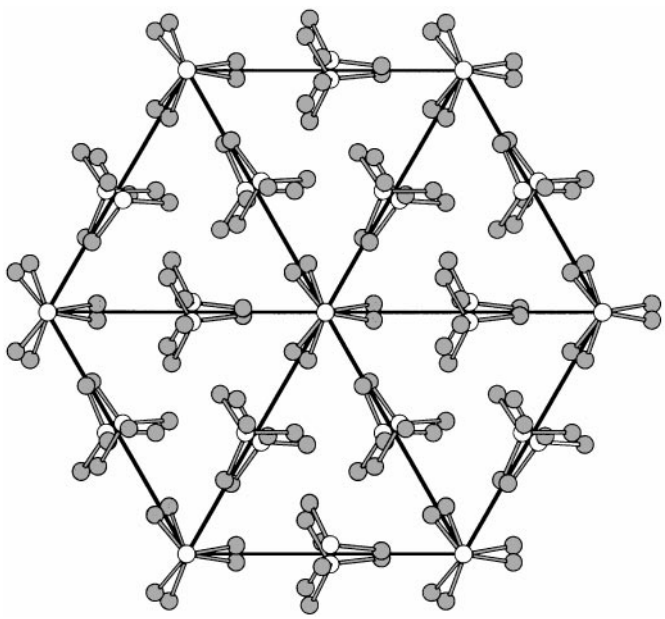

FIG. 2. $[PSe_4]^{3-}$ tetrahedral anions of $Na_{1.5}Pb_{0.75}PSe_4$ viewed down the body diagonal of the unit cell. It is easy to see how the structure is noncentrosymmetric because all of the tetrahedra are pointing in the same direction. The P atoms are shown in white, while the Se atoms are shown in gray.

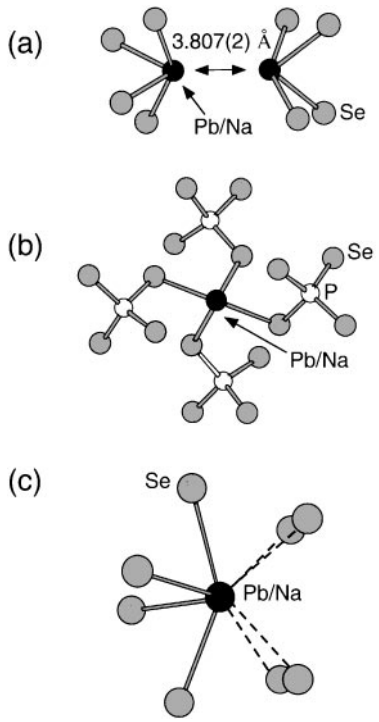

FIG. 3. Environment of cation site A. This position is occupied by 50% Pb and 50% Na in the case of $Na_{1.5}Pb_{0.75}PSe_4$ (this position is occupied by 100% Pb in the case of $Na_{0.5}Pb_{1.75}GeS_4$ or $Li_{0.5}Pb_{1.75}GeS_4$). (A) A distance of approximately 3.8 Å between symmetry-equivalent atoms allows for a close contact. (In the case where this position is occupied by only Pb atoms, this distance can be considered a Pb–Pb lone pair interaction.) (B) View of the tetrahedral $[PSe_4]^{3-}$ units coordinated to the cation site A position. (C) There are four long A–chalcogen interactions, shown with dotted lines.

occupied by Na(2) or Li(2) but only as 4-coordinate if occupied by Pb(2). See Tables 4 and 5 for additional bond lengths and angles.

Perhaps it is not surprising that Na and Pb cations occupy the same crystallographic sites in these structures.

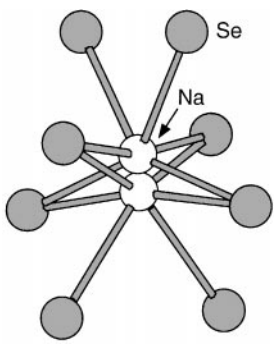

FIG. 4. View of cation site B. This site is a distorted 8-coordinate pocket occupied by 50% Na in $Na_{1.5}Pb_{0.75}PSe_4$. (This site is occupied by 33.3% Na/Li and 16.7% Pb in $Na_{0.5}Pb_{1.75}GeS_4$ and $Li_{0.5}Pb_{1.75}GeS_4$.) This position generates a symmetry-equivalent atom ca. 1 Å from itself, thus it can only be 50% occupied at the most.

TABLE 4
Selected Distances (Å) for $Na_{1.5}Pb_{0.75}PSe_4$, $Na_{0.5}Pb_{1.75}GeS_4$, and $Li_{0.5}Pb_{1.75}GeS_4$

Distances	$Na_{1.5}Pb_{0.75}PSe_4$	$Na_{0.5}Pb_{1.75}GeS_4$	$Li_{0.5}Pb_{1.75}GeS_4$
$M(1)$–$Q(1)$	2.228(3)	2.238(2)	2.244(4)
$M(1)$–$Q(2)$	2.212(1) × 3	2.214(2) × 3	2.209(2) × 3
$A(1)$–$Q(1)$	2.9124(3) × 2	2.867(2) × 2	2.828(2) × 2
$A(1)$–$Q(2)$	3.054(1) × 2	2.846(2) × 2	2.8623(6) × 2
$A(1)$–$Q(2)$	3.4017(9) × 2	3.443(2) × 2	3.403(2) × 2
$A(1)$–$Q(2)$	3.4385(9) × 2	3.455(2) × 2	3.508(3) × 2
$A(1)$–$A(1)$	3.807(2)	3.856(3)	3.716(1)
$A(1)$–$B(2)$	3.847(3) × 2	3.750(3) × 2	3.728(1) × 2
$B(2)$–$Q(2)$	2.936(1) × 2	2.806(2) × 2	2.601(3) × 2
$B(2)$–$Q(2)$	3.139(3) × 2	2.860(4) × 2	2.860(4) × 2
$B(2)$–$Q(2)$	3.381(6) × 2	3.315(3) × 2	3.496(4) × 2
$B(2)$–$Q(2)$	4.052(6) × 2	3.716(1) × 2	4.308(4) × 2
$B(2)$–$B(2)$	0.81(1)	1.021(4)	0.968(6)

Note. A = cation site A (this site is occupied by 50% Na and 50% Pb for $Na_{1.5}Pb_{0.75}PSe_4$ or by only Pb in the case of $Na_{0.5}Pb_{1.75}GeS_4$ and $Li_{0.5}Pb_{1.75}GeS_4$); B = cation site B (this site is occupied by 50% Na for $Na_{1.5}Pb_{0.75}PSe_4$ or by 16.7% Na/Li and 33.3% Pb in the case of $Na_{0.5}Pb_{1.75}GeS_4$ and $Li_{0.5}Pb_{1.75}GeS_4$); M = P or Ge; Q = S or Se.

The effective ionic radius for Na^+ with a coordination number of 8 is 1.18 Å, whereas that of Pb^{2+} in the same coordination environment is 1.29 Å (44). The difference is only 0.11 Å. However, in order to be certain, we chose the structure determination of $Na_{0.5}Pb_{1.75}GeS_4$ to be tested for possible twinning. All cubic ($I\bar{4}2d$ and $I2_13$) and trigonal ($R3c$) subgroups were considered, but none could lead to a coherent ordering with reasonable atomic displacement parameters. Also, despite extensive attempts on many single-crystal samples we could not confirm the existence of a superstructure.

The effective ionic radius for Li^+ with a coordination number of 8 is 0.92 Å, which is 0.37 Å smaller than Pb^{2+} (44). With this in mind, we collected crystallographic data for $Li_{0.5}Pb_{1.75}GeS_4$ out to 61.05° 2θ to obtain higher-resolution data. In addition, we collected the data at 60 s per frame in order to catch any possible superstructure reflections. No super cell was observed, and thus no ordering of the Li and Pb cations was found.

In comparison to $Ba_3CdSn_2S_8$ (30), the structure of the three compounds reported here is only slightly different. Table 6 shows the relationship between the compounds reported here and those from Ref. (30). The main difference is that the Cd site (cation site B) in $Ba_3CdSn_2S_8$ is a special position, 12*b*, while in the compounds reported here cation site B is a 24*d* position, which can have a maximum occupancy of 50% owing to the presence of a short distance to a symmetry-equivalent position. Simply, site B is shifted to a lower-symmetry position on going from $Ba_3CdSn_2S_8$ to

TABLE 5
Selected Intramolecular Angles (deg) for $Na_{1.5}Pb_{0.75}PSe_4$, $Na_{0.5}Pb_{1.75}GeS_4$, and $Li_{0.5}Pb_{1.75}GeS_4$

Angles	$Na_{1.5}Pb_{0.75}PSe_4$	$Na_{0.5}Pb_{1.75}GeS_4$	$Li_{0.5}Pb_{1.75}GeS_4$
$Q(1)-M(1)-Q(2)$	107.14(8) × 3	105.40(8) × 3	105.39(7) × 3
$Q(2)-M(1)-Q(2)$	111.70(8) × 3	113.21(8) × 3	113.23(6) × 3
$Q(1)-A(1)-Q(1)$	144.32(5)	149.28(5)	147.09(9)
$Q(1)-A(1)-Q(2)$	82.80(3) × 2	86.62(5) × 2	85.89(9) × 2
$Q(1)-A(1)-Q(2)$	71.40(2) × 2	71.78(5) × 2	72.21(6) × 2
$Q(2)-A(1)-Q(2)$	87.01(4)	90.89(6)	96.5(1)
$Q(2)-B(2)-Q(2)$	166.6(3)	170.4(1)	169.0(2)
$Q(2)-B(2)-Q(2)$	145.2(2)	147.9(9)	148.08(8)
$Q(2)-B(2)-Q(2)$	136.6(2)	131.6(1)	129.5(2)
$Q(2)-B(2)-Q(2)$	98.7(1)	98.42(8)	98.17(9)
$Q(2)-B(2)-Q(2)$	92.48(4)	91.97(6)	92.34(4)
$Q(2)-B(2)-Q(2)$	76.9(2)	78.55(6)	80.25(8)
$Q(2)-B(2)-Q(2)$	76.02(5)	75.42(8)	74.3(1)
$Q(2)-B(2)-Q(2)$	70.4(2)	73.78(7)	72.8(1)

Note. A = cation site A (this site is occupied by 50% Na and 50% Pb for $Na_{1.5}Pb_{0.75}PSe_4$ or by only Pb in the case of $Na_{0.5}Pb_{1.75}GeS_4$ and $Li_{0.5}Pb_{1.75}GeS_4$); B = cation site B (this site is occupied by 50% Na for $Na_{1.5}Pb_{0.75}PSe_4$ or by 16.7% Na/Li and 33.3% Pb in the case of $Na_{0.5}Pb_{1.75}GeS_4$ and $Li_{0.5}Pb_{1.75}GeS_4$); M = P or Ge; Q = S or Se.

the compounds reported here, resulting in a more distorted coordination geometry, since Li^+, Na^+, or Pb^{2+} needs more contacts to satisfy its bond valence sums.

Spectroscopy

The transparent, well-formed crystals of $Na_{1.5}Pb_{0.75}PSe_4$ and $Na_{0.5}Pb_{1.75}GeS_4$ were suitable for single-crystal optical transmission measurements. Both compounds exhibit sharp optical absorptions of 2.09 and 2.08 eV respectively, see Fig. 5. Crystals of $Li_{0.5}Pb_{1.75}GeS_4$ were not transparent enough for single-crystal measurements, so instead the solid-state UV/vis diffuse reflectance spectrum was obtained, which gave a band gap of 1.95 eV, see Fig. 5. This is 0.13 eV smaller than the Na analogue which is to be expected since the interactions between Li and S are more covalent than those of Na and S.

The far-IR spectra of all three compounds are shown in Fig. 6. The spectrum of $Na_{1.5}Pb_{0.75}PSe_4$ displays two strong absorptions at $\sim$430 and 408 cm^{-1}. These vibrations can be assigned to $[PSe_4]^{3-}$ asymmetric stretching modes and are diagnostic in distinguishing the tetrahedral selenophosphate ligand from other ligands such as the ethane-like, P_2Se_6 ligand (10). Also, there is a broad absorption around 218 cm^{-1} which is probably associated with Pb–Se vibrations. In $Na_{0.5}Pb_{1.75}GeS_4$, and $Li_{0.5}Pb_{1.75}GeS_4$ the far-IR spectra are almost identical. The spectra display two strong absorptions at $\sim$395 and 362 cm^{-1}, which correspond to $[GeS_4]^{4-}$ asymmetric stretching vibrations. The absorptions at lower wavenumbers, 252 and 232 cm^{-1}, should correspond to Pb–S vibrations.

Raman spectra for all three compounds are shown in Fig. 7. One can see that the Raman spectra for $Na_{0.5}Pb_{1.75}GeS_4$ and $Li_{0.5}Pb_{1.75}GeS_4$ are almost identical, whereas the spectrum for $Na_{1.5}Pb_{0.75}PSe_4$ is more spread out but still has the same features. We can attribute the peaks around 250 cm^{-1} and below to Pb–S or Pb–Se stretches. Since the Pb–Se vibration involves the heavier of the two chalcogens, the peaks below 250 cm^{-1} appear at lower cm^{-1} for $Na_{1.5}Pb_{0.75}PSe_4$ than for $Na_{0.5}Pb_{1.75}GeS_4$ and $Li_{0.5}Pb_{1.75}GeS_4$. The three stretches at higher cm^{-1} should correspond to Ge–S or P–Se bonding interactions. More specifically, the presence of the Raman peak at 442 cm^{-1} for $Na_{1.5}Pb_{0.75}PSe_4$ and ca. 408 cm^{-1} for the thiogermanates is attributed to the symmetric stretching

TABLE 6
Comparison of $A_6B_3M_4Q_{16}$ Structures

A_6	B_3[a]	M_4	Q_{16}	Empirical formula ($Z = 4$)	
$(Ba^{2+})_6$	$(Cd^{2+})_2\square$	$(Sn^{4+})_4$	$(S^{2-})_{16}$	$Ba_6(Cd_2\square)Sn_4S_{16}$	$Ba_6Cd_2(SnS_4)_4$ (30)[b]
$(Ba^{2+})_6$	$Ag_2(Cd^{2+})$	$(Sn^{4+})_4$	$(S^{2-})_{16}$	$Ba_6(Ag_2Cd)Sn_4S_{16}$	$Ba_6Ag_2Cd(SnS_4)_4$ (30)[c]
$(Na^+)_3(Pb^{2+})_3$	$(Na^+)_3$	$(P^{5+})_4$	$(Se^{2-})_{16}$	$(Na_3Pb_3)(Na_3)P_4Se_{16}$	$Na_6Pb_3(PSe_4)_4$
$(Pb^{2+})_6$	$(Na^+)_2(Pb^{2+})$	$(Ge^{4+})_4$	$(S^{2-})_{16}$	$(Pb_6)(Na_2Pb)Ge_4S_{16}$	$Na_2Pb_7(GeS_4)_4$
$(Pb^{2+})_6$	$(Li^+)_2(Pb^{2+})$	$(Ge^{4+})_4$	$(S^{2-})_{16}$	$(Pb_6)(Li_2Pb)Ge_4S_{16}$	$Li_2Pb_7(GeS_4)_4$

[a] Site B for the first two compounds is a 12*b* position; however, site B for the last three compounds is a 24*d* position, which can only have a maximum occupancy of 50% owing to the presence of a short distance to a symmetry-equivalent position.

[b] The authors allowed the Ba and Cd sites to refine freely and obtained the formula of $Ba_{2.82}Cd_{1.05}Sn_2S_8$, where the 24*d* position is 94% occupied by Ba and the 12*b* site is 70% occupied by Cd. No constraint was added to the refinement to make the formula charge balance. Therefore, $Ba_3CdSn_2S_8$ or $Ba_6Cd_2Sn_4S_{16}$ can be considered as an idealized formula.

[c] For the compound $Ba_6Ag_2CdSn_4S_{16}$ it was proposed that the 24*d* position is fully occupied by Ba and that the 12*b* site is occupied 66.67% by Ag and 33.33% by Cd. However, only a powder pattern was obtained, and no single-crystal structure determination was performed.

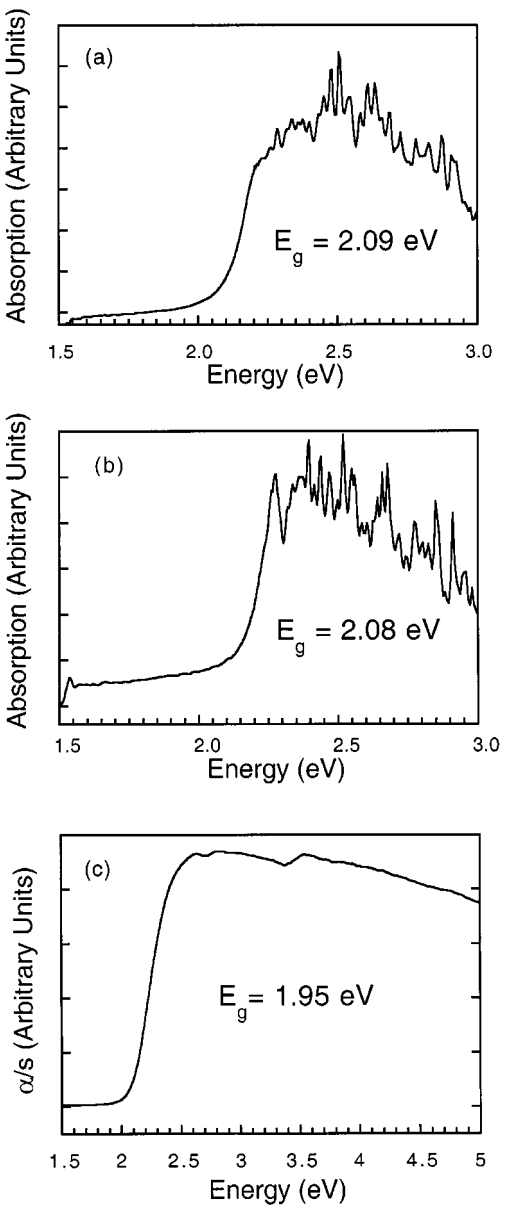

FIG. 5. Single-crystal optical spectra of (A) $Na_{1.5}Pb_{0.75}PSe_4$ and (B) $Na_{0.5}Pb_{1.75}GeS_4$. (C) Optical spectrum obtained from a polycrystalline powdered sample of $Li_{0.5}Pb_{1.75}GeS_4$.

vibrations of the $[PSe_4]^{3-}$ and $[GeS_4]^{4-}$ tetrahedra, respectively. Since the average atomic number of Ge–S is greater than that of P–Se, the Ge–S stretches in $Na_{0.5}Pb_{1.75}GeS_4$ and $Li_{0.5}Pb_{1.75}GeS_4$ occur at a lower cm^{-1} than those of the P–Se in $Na_{1.5}Pb_{0.75}PSe_4$. Table 7 lists the most important Raman and far-IR spectroscopic absorption peaks for all three compounds.

Nonlinear Optical (NLO) Behavior

Preliminary experiments on powder samples of $Na_{0.5}Pb_{1.75}GeS_4$ using $\sim$150 μJ laser light at 3.5 μm from the sample (45) showed a second harmonic generation (SHG) signal which was 7 to 8 times greater than that observed for similarly prepared powder samples of $LiNbO_3$. The presence of SHG is consistent with the current cubic space group and crystal class ($\bar{4}3m$) (46). Further experiments are needed to characterize the NLO behavior (47).

CONCLUDING REMARKS

All three compounds reported here are isostructural to one another and crystallize in the cubic, noncentrosymmetric space group $I\bar{4}3d$ with a structure similar to that of $Ba_3CdSn_2S_8$. This structure seems to be quite stable and

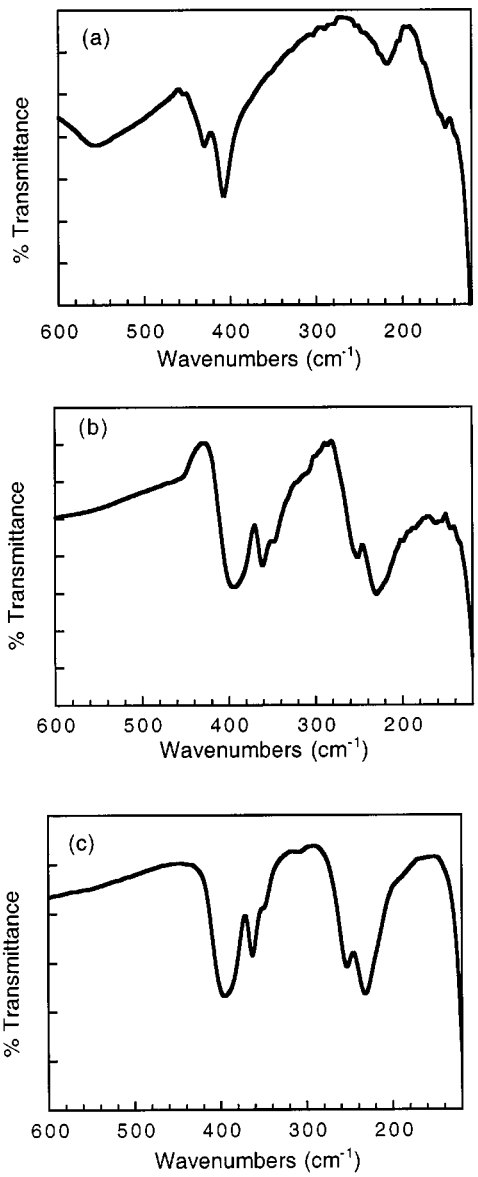

FIG. 6. Far-IR spectra of (A) $Na_{1.5}Pb_{0.75}PSe_4$, (B) $Na_{0.5}Pb_{1.75}GeS_4$, and (C) $Li_{0.5}Pb_{1.75}GeS_4$.

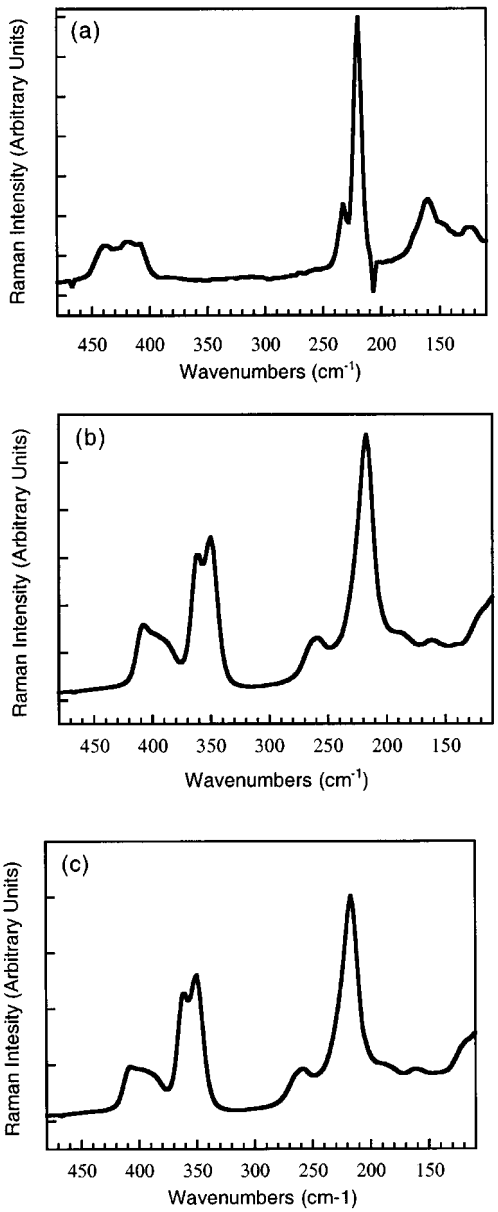

FIG. 7. Raman spectra of (A) $Na_{1.5}Pb_{0.75}PSe_4$, (B) $Na_{0.5}Pb_{1.75}GeS_4$, and (C) $Li_{0.5}Pb_{1.75}GeS_4$.

flexible since it tolerates disorder and/or vacancies (see Table 6). It is also remarkable that the structure can be formed with $[PSe_4]^{3-}$, $[GeS_4]^{4-}$, or $[SnS_4]^{4-}$ tetrahedra, since the charges of these building blocks are different. This happens because of the ability of both cation site A and B to accommodate $+1$ or $+2$ metals alone or simultaneously by introducing disorder and/or vacancies. The amount of disorder and/or vacancies is adjusted based on the charge-balancing requirements of the particular tetrahedral unit ($[PSe_4]^{3-}$, $[GeS_4]^{4-}$, or $[SnS_4]^{4-}$). Table 6 can be used to predict other quaternary and quinary compounds, which

TABLE 7
Infrared and Raman Data (cm^{-1}) for $Na_{1.5}Pb_{0.75}PSe_4$, $Na_{0.5}Pb_{1.75}GeS_4$, and $Li_{0.5}Pb_{1.75}GeS_4$

$Na_{1.5}Pb_{0.75}PSe_4$		$Na_{0.5}Pb_{1.75}GeS_4$		$Li_{0.5}Pb_{1.75}GeS_4$	
IR	Raman	IR	Raman	IR	Raman
	442 w		408 m		408 m
430 m		394 vs	392 w	395 vs	392 w
	418 w	361 m	363 s	363 m	362 s
408 vs	409 w	346 w	350 s	349 w	350 s
	232 m		261 w		260 w
		252 m		253 m	
218 m		232 vs		232 vs	
	221 vs		216 vs		216 vs
	160 m		188 vw		188 vw
	124 w		161 vw		161 vw

Note. vs = very strong, s = strong, m = medium, w = weak, vw = very weak.

may form with this structure type. Synthetic investigations into the existence of some predictable formulas are worthwhile (48) since $Na_{0.5}Pb_{1.75}GeS_4$ shows interesting properties. Preliminary measurements of the second harmonic generation signal of polycrystalline powder samples of $Na_{0.5}Pb_{1.75}GeS_4$ indicate that this compound could be a potential NLO material. Further investigations are necessary to explore the NLO behavior.

ACKNOWLEDGMENTS

Financial support from the National Science Foundation (Grant DMR-9817287) is gratefully acknowledged. This work made use of the SEM facilities of the Center for Electron Optics at Michigan State University. The Bruker SMART platform CCD diffractometer at Michigan State University was purchased with funds from the National Science Foundation (CHE-9634638). We acknowledge the use of the W. M. Keck Microfabrication Facility at Michigan State University, a NSF MRSEC facility. In addition, we acknowledge the Animal Health Diagnostic Laboratory in the College of Veterinary Medicine at Michigan State University for the ICP measurements. We gratefully acknowledge our collaborators at Rockwell International (M. Rosker and M. Eubank) for the NLO measurements.

REFERENCES

1. M. G. Kanatzidis, *Chem. Mater.* **2,** 353–363 (1990).
2. M. G. Kanatzidis and A. C. Sutorik, *Prog. Inorg. Chem.* **43,** 151–265 (1995).
3. S. A. Sunshine, D. Kang, and J. A. Ibers, *J. Am. Chem. Soc.* **109,** 6202–6204 (1987).
4. J. A. Cody, M. F. Mansuetto, S. Chien, and J. A. Ibers, *Mater. Sci. Forum* **35,** 152–153 (1994).
5. M. G. Kanatzidis, *Curr. Opin. Solid State Mater. Sci.* **2**(2), 139–149 (1997) and references therein.
6. K. Chondroudis and M. G. Kanatzidis, *Inorg. Chem.* **34,** 5401–5402 (1995).

7. K. Chondroudis and M. G. Kanatzidis, *J. Chem. Soc., Chem. Commun.* 1371–1372 (1996).
8. K. Chondroudis, M. G. Kanatzidis, J. Sayettat, S. Jobic, and R. Brec, *Inorg. Chem.* **36,** 5859–5868 (1997).
9. G. Gauthier, S. Jobic, R. Brec, and J. Rouxel, *Inorg. Chem.* **37**(10), 2332–2333 (1998).
10. T. J. McCarthy and M. G. Kanatzidis, *Inorg. Chem.* **34,** 1257–1267 (1995).
11. K. Chondroudis, T. M. McCarthy, and M. G. Kanatzidis, *Inorg. Chem.* **35,** 840–844 (1996).
12. K. Chondroudis, J. A. Hanko, and M. G. Kanatzidis, *Inorg. Chem.* **36,** 2623–2632 (1997).
13. K. Chondroudis and M. G. Kanatzidis, *J. Solid State Chem.* **138,** 321–328 (1998).
14. K. Chondroudis and M. G. Kanatzidis, *J. Solid State Chem.* **136,** 79–86 (1998).
15. T. J. McCarthy and M. G. Kanatzidis, *Chem. Mater.* **5,** 1061–1063 (1993).
16. T. J. McCarthy and M. G. Kanatzidis, *J. Chem. Soc., Chem. Commun.* 1089–1090 (1994).
17. J. H. Chen, P. K. Dorhout, and J. E. Ostenson, *Inorg. Chem.* **35,** 5627–5633 (1996).
18. J. H. Chen and P. K. Dorhout, *Inorg. Chem.* **34,** 5705–5706 (1995).
19. J. A. Aitken, K. Chondroudis, V. G. Young, Jr., and M. G. Kanatzidis, *Inorg. Chem.* **39,** 1525–1533 (2000).
20. K. Chondroudis and M. G. Kanatzidis, *J. Am. Chem. Soc.* **119,** 2574–2575 (1997).
21. P. K. Dorhout and T. M. Malo, *Z. Anorg. Allg. Chem.* **622,** 385–391 (1996).
22. P. M. Bridenbaugh, *Mater. Res. Bull.* **8,** 1055–1060 (1973).
23. C. D. Carpentier and R. Nitche, *Mater. Res. Bull.* **9,** 1097–1100 (1974).
24. G. Ouvrard, R. Brec, and J. Rouxel, *Mater. Res. Bull.* **20,** 1181–1189 (1985).
25. A. N. Volodina, T. B. Koubchinova, S. I. Maximova, E. N. Mouraviev, C. A. Niazov, and N. I. Tchibiskova, *Zh. Neorg. Khim. SSSR* **32,** 2899 (1987).
26. G. A. Marking and M. G. Kanatzidis, *J. Alloys Compd.* **259,** 122–128 (1997).
27. G. A. Marking, J. A. Hanko, and M. G. Kanatzidis, *Chem. Mater.* **10,** 1191–1199 (1998).
28. J.-H. Liao and M. G. Kanatzidis, *Chem. Mater.* **5,** 1561–1569 (1993).
29. G. A. Marking and M. G. Kanatzidis, manuscript in preparation.
30. C. L. Teske, *Z. Anorg. Allg. Chem.* **522,** 122–130 (1985).
31. F. Feher, "Handbuch der präparativen anorganischen Chemie" (G. Brauer, Ed.), pp. 280–281. Ferdinand Enke, Stuttgart, Germany, 1954.
32. J. A. Aitken, J. A. Cowen, and M. G. Kanatzidis, *Chem. Mater.* **10,** 3928–3935 (1998).
33. "CERIUS^2," Version 2.0. Molecular Simulations Inc., Cambridge, England, 1995.
34. (a) W. W. Wendlandt and H. G. Hecht, "Reflectance Spectroscopy." Interscience Publishers, New York, 1966. (b) G. Kotüm, "Reflectance Spectroscopy." Springer-Verlag, New York, 1969. (c) S. P. Tandon and J. P. Gupta, *Phys. Status Solidi* **38,** 363–367 (1970).
35. "SMART and SAINT. Data Collection and Processing Software for the SMART System." Bruker Analytical X-ray Instruments Inc., Madison, WI, 1995.
36. G. M. Sheldrick, University of Gottingen, Germany, to be published.
37. "SHELXTL V-5." Siemens Analytical X-ray Systems Inc., Madison, WI.
38. V. Petricek, and M. Dusek, "JANA98: Programs for Modulated and Composite Crystals." Institute of Physics, Prague, Czech Republic, 1998.
39. "Stoe X-Shape: Crystal Optimisation for Numerical Absorption Correction." STOE & Cie GmbH, Darmstadt, Germany, 1996.
40. K. Chondroudis and M. G. Kanatzidis, *Inorg. Chem. Commun.* **1/2,** 55–57 (1998).
41. K. Chondroudis and M. G. Kanatzidis, *Inorg. Chem.* **37**(15), 3792–3797 (1998).
42. K. Chondroudis and M. G. Kanatzidis, *J. Chem. Soc. Chem. Commun.* 401–402 (1997).
43. J. R. Gavarri, J. P. Vigouroux, and G. Calvarin, *J. Solid State Chem.* **36,** 81–90 (1981).
44. R. D. Shannon, *Acta. Crystallogr.* **A32,** 751–767 (1976).
45. M. J. Rosker and H. O. Marcy, "Novel Optical Materials and Applications" (I. Khoo, F. Simoni, and C. Umelon, Eds.), pp. 198–203. Wiley, New York, 1997.
46. T. Hahn, "International Tables for X-ray Crystallography," 4th revised ed., Vol. A, p. 788. Kluwer Academic Publishers, Boston, 1996.
47. M. J. Rosker, M. Eubank, M. Evain, G. A. Marking, and M. G. Kanatzidis, unpublished results.
48. J. A. Aitken and M. G. Kanatzidis, work in progress.